SCIENTIFIC REPORTS

OPEN

SUBJECT AREAS:
SECONDARY METABOLISM
PLANT MOLECULAR BIOLOGY
BACTERIOLOGY
BIOTIC

Received
22 November 2013

Accepted
31 January 2014

Published
17 February 2014

Correspondence and requests for materials should be addressed to S.N. (anamba@mail.ecc.u-tokyo.ac.jp)

Purple top symptoms are associated with reduction of leaf cell death in phytoplasma-infected plants

Misako Himeno, Yugo Kitazawa, Tetsuya Yoshida, Kensaku Maejima, Yasuyuki Yamaji, Kenro Oshima & Shigetou Namba

Graduate School of Agricultural and Life Sciences, The University of Tokyo, 1-1-1 Yayoi, Bunkyo-ku, Tokyo 113-8657, Japan.

Plants exhibit a wide variety of disease symptoms in response to pathogen attack. In general, most plant symptoms are recognized as harmful effects on host plants, and little is known about positive aspects of symptoms for infected plants. Herein, we report the beneficial role of purple top symptoms, which are characteristic of phytoplasma-infected plants. First, by using plant mutants defective in anthocyanin biosynthesis, we demonstrated that anthocyanin accumulation is directly responsible for the purple top symptoms, and is associated with reduction of leaf cell death caused by phytoplasma infection. Furthermore, we revealed that phytoplasma infection led to significant activation of the anthocyanin biosynthetic pathway and dramatic accumulation of sucrose by about 1000-fold, which can activate the anthocyanin biosynthetic pathway. This is the first study to demonstrate the role and mechanism of the purple top symptoms in plant–phytoplasma interactions.

Phytoplasmas are plant-pathogenic bacteria that inhabit phloem sieve elements in host plants, and belong to the class *Mollicutes*[1,2]. Phytoplasmas are transmitted between plants by phloem-feeding insects belonging to the order Hemiptera. Plants infected with phytoplasmas exhibit a variety of symptoms, including stunted growth, yellowed foliage, purple top (reddening), witches' blooms (proliferation of branches and leaves), virescence (development of green flowers and the loss of pigments), and phyllody (conversion of flowers into leaves)[2,3]. A number of mechanisms by which phytoplasmas induce disease symptoms have been proposed to date. Phytoplasma-secreted proteins, or so-called effectors, are predicted to play important roles in host-parasite interactions and pathogenicity, and to cause disease symptoms[4]. In fact, some phytoplasma effectors have been identified as inducers of witches' bloom symptoms or leaf-like flower development[5–7]. On the other hand, stunting and yellowing induced by phytopathogenic mollicutes can be associated with the utilization of sugars in the phloem[8]. It has been shown that *Spiroplasma citri*, which also belongs to the class *Molllicutes* and is restricted to the cytoplasm of phloem cells in plants, preferentially utilizes fructose and leads to abnormally high glucose concentrations in the phloem, resulting in symptoms such as yellowing and stunting[9]. On the other hand, the mechanism causing purple coloration of leaves, or so-called "purple top", which is characteristic of phytoplasma-infected potato, grapevine, corn, maize, and clover[1,10–13], is still largely unknown.

Anthocyanins are plant secondary metabolites synthesized by the flavonoid pathway, and play important roles in flower pigmentation, allelopathy, or UV protection[14,15]. They are also important as antioxidant molecules to protect plant cells against damage by reactive oxygen species[16–18]. Indeed, the production of anthocyanins in autumn leaves reduces the risk of photo-oxidative damage and delays leaf senescence[19,20]. Anthocyanin biosynthesis genes have been identified in several plant species, including *Arabidopsis thaliana* and *Petunia hybrida*[14,21,22]. The biosynthetic pathway for anthocyanin production can be divided into upstream and downstream sections[23]. Chalcone synthase (CHS), one key enzyme in the upstream reactions, is responsible for the first step committed to flavonoid synthesis. Dihydroflavonol 4-reductase (DFR) serves within the downstream section to synthesize anthocyanin derivative molecules. In the *Arabidopsis* genome, most flavonoid pathway genes including *CHS* and *DFR* are present as single copies[14]. Therefore, in *Arabidopsis* both *chs* and *dfr* mutants are completely devoid of anthocyanins[14]. Anthocyanin accumulation is regulated by various environmental factors, such as light, temperature, nutrient, and osmotic stress[24–26]. It has been reported that anthocyanin biosynthesis genes including *CHS* and *DFR* are induced in a sucrose-dependent manner[27,28].

Flavonoids, including anthocyanins, are recognized as a significant contributor to plant defense against microbial pathogens[15]. Flavonoid induction in response to pathogen attack has been reported in grapevine and poplar[29,30]. Recently, global transcription profiles in grapevine infected with Bois noir phytoplasma have revealed that the genes involved in the flavonoid biosynthetic pathway are up-regulated in phytoplasma-infected leaves[31,32]. However, the roles of anthocyanins and their biosynthesis genes in the phytoplasma-infected plants are not clear.

In the present study, we demonstrate the induction of anthocyanin biosynthesis in response to an infection by '*Candidatus* Phytoplasma asteris' OY-W strain (OY-W phytoplasma). By using anthocyanin-deficient *Arabidopsis* mutants, we examined the effects of anthocyanin accumulation on leaf cell death and phytoplasma propagation. Furthermore, we investigated the concentrations of several sugars in phytoplasma-infected plants and discuss the relationships between sucrose content and purple top symptoms during OY-W phytoplasma infection.

Results

Distribution of phytoplasma in purple colored leaves. The infection by OY-W phytoplasma induced purple discoloration in *Arabidopsis* and *Petunia* plants (Fig. 1). In the OY-W infected *Arabidopsis*, the lower, rather than the upper, surface of rosette leaves turned almost entirely purple within 1 to 2 weeks following inoculation (Fig. 1a, 1b). Similarly, the OY-W infected *Petunia* (cv. Vakara Blue) exhibited foliar purple discoloration beginning 3 to 4 weeks after inoculation (Fig. 1c).

Phytoplasmas generally inhabit phloem elements in plants. However, in infected *Petunia* leaves, purple coloration was observed along leaf margins around midveins rather than along midveins (Fig. 1c). We investigated the relationships between the area of purple-pigmentation and phytoplasma localization. First, *Petunia* leaves that exhibited purple coloration were divided into three tissues (midveins, pigmentation area, and other non-pigmentation area), and the phytoplasma populations therein were quantified using real-time PCR. As a result, phytoplasma accumulation in the midveins was significantly high compared with other tissues, whereas there was no significant difference between tissues with and without pigmentation (Fig. 1d). This suggests that OY-W phytoplasma accumulated mainly along the veins in *Petunia* leaves. Moreover, this result suggests that the purple coloration was not related to the localization of phytoplasma.

The activation of anthocyanin biosynthesis by OY-W phytoplasma infection. To test the hypothesis that phytoplasma-induced purple pigmentation is due to anthocyanin accumulation by host plants, *chs* mutant plants, which are anthocyanin deficient, were inoculated with OY-W phytoplasma. After 10 days post-inoculation, wild-type leaves showed full purple coloration (Fig. 1a, 1b), while *chs* leaves showed a little yellowing at leaf tips but did not show purple-colored symptoms (Fig. 2a). This suggests that the phytoplasma-induced purple top symptoms resulted from ectopic anthocyanin accumulation.

To examine whether OY-W phytoplasma infection activates the anthocyanin biosynthetic pathway, we quantified mRNA accumulation of the early and late anthocyanin biosynthetic genes, *CHS* and *DFR*, respectively, in the leaves of *Arabidopsis* and *Petunia* plants exhibiting purple-coloration symptoms. *CHS* expression was increased significantly by 8.8- and 3.1-fold in infected *Arabidopsis* and *Petunia*, respectively, compared to healthy controls (Fig. 2b, upper panels). *DFR* transcripts were also greatly increased in both infected plants, especially in the OY-W–infected *Petunia*, by 24-fold (Fig. 2b, lower panels). These results suggested that OY-W phytoplasma infection strongly induces the expression of both early and late anthocyanin biosynthetic genes in both *Arabidopsis* and *Petunia*.

Reduction of cell death in leaves accumulated with anthocyanin. To investigate the roles of anthocyanin accumulation in phytoplasma-infected leaves, we compared symptoms between two OY-W–infected *Petunia* cultivars, Vakara Blue, which blooms with blue flowers and exhibits purple-colored leaves during phytoplasma infection (Fig. 1c), and Vakara White, which blooms with white flowers and has defects in the anthocyanin biosynthesis pathway. After 4 weeks post-inoculation, the OY-W–infected Vakara Blue exhibited foliar purple coloration along leaf margins; however, the leaves of Vakara White did not exhibit purple coloration, and instead showed yellowing from the leaf edges (Fig. 3f). Furthermore, infected leaves of Vakara White appeared to undergo accelerated senescence compared with those of Vakara Blue (Fig. 3b, 3f). In fact, we often observed necrosis of the leaf margins in the infected leaves of Vakara White (Fig. 3f). To examine the relationship between purple coloration and necrosis of leaf margins during phytoplasma infection, we identified dead cells in *Petunia* plants using trypan blue staining. The leaf margins of OY-W–infected Vakara White were strongly stained dark blue (Fig. 3h), while those of Vakara Blue were not stained (Fig. 3d). This suggests that cell death was induced by

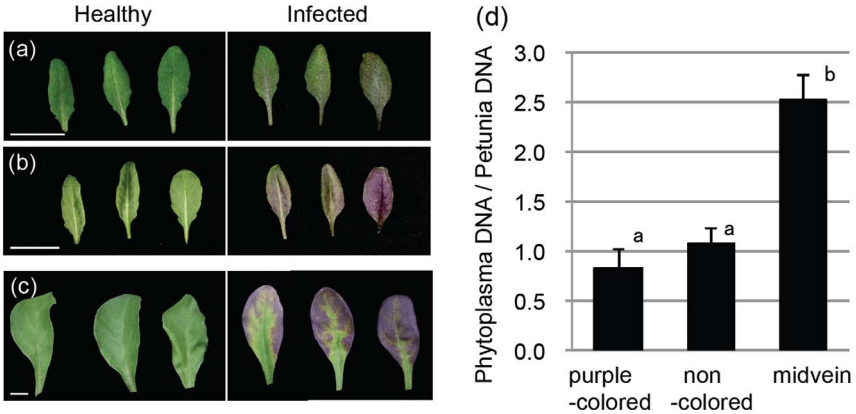

Figure 1 | Purple top symptom and phytoplasma distribution. Typical samples of OY-W-infected leaves exhibiting purple coloration symptom in *Arabidopsis* wild-type (a, b) and *Petunia* Vakara Blue (c). The leaves were healthy (each three leaves in left sides) and infected with OY-W phytoplasma (each three leaves in right sides). (a) shows upper surface of rosette leaves of *Arabidopsis*, and (b) shows lower surface. Bars = 1 cm. (d) Phytoplasma accumulation in *Petunia* leaves exhibiting purple coloration symptoms. *Petunia* leaves exhibiting symptoms were divided into three tissues; midveins, purple-colored leaf margins (purple-colored), and other non-colored leaf margins (non-colored). OY-W populations were estimated by real-time PCR for OY-W *tufB* gene. Each bar represents the average of three biological replicates (±SE). *P. hybrida* glyceraldehyde-3-phosphate dehydrogenase gene (*PhGAPDH*) was used for normalization. Different alphabets indicate significant differences between them ($P < 0.05$).

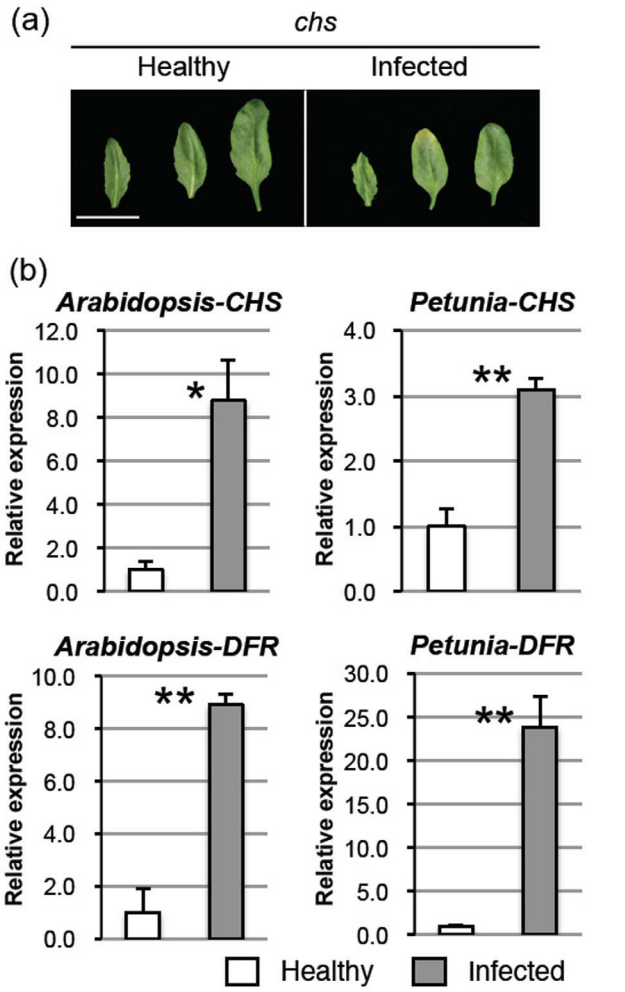

Figure 2 | Purple top symptom is due to plant anthocyanin biosynthesis. (a) Typical samples of healthy and OY-W infected rosette leaves of *Arabidopsis chs* mutant. Experimental conditions on phytoplasma-infection and observation were the same to Fig. 1a, b. Bar = 1 cm. (b) Expression analyses of anthocyanin synthesis genes, *CHS* and *DFR*, in *Arabidopsis* and *Petunia*. Transcriptional levels were obtained by qRT-PCR in healthy and OY-W-infected leaves. Each bar represents the average of three biological replicates(±SE). The average expression levels of healthy leaves were set as 1.0. Significant differences between healthy and infected leaves are indicated as * ($P < 0.05$) or ** ($P < 0.01$).

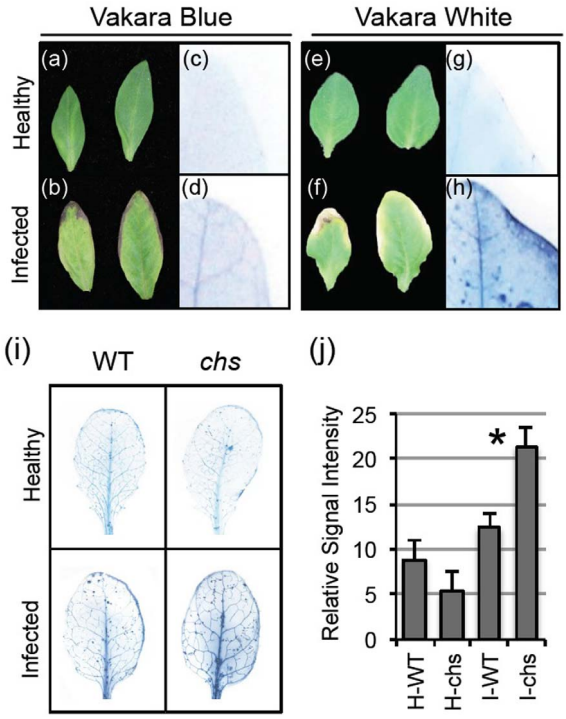

Figure 3 | Anthocyanin accumulation reduces cell death in *Petunia* and *Arabidopsis*. (a–h) Differences in disease symptoms between two *Petunia* cultivars, Vakara Blue and Vakara White. (i) Trypan blue staining assays in healthy and OY-W infected *Arabidopsis* wild type and *chs* mutant. The values of signal intensity detected by trypan blue staining were calculated by image J. The relative signal intensities are means of 3 samples, with standard error of the mean. Significant difference between infected WT and infected *chs* is indicated as * ($P < 0.05$).

OY-W phytoplasma infection along leaf margins in Vakara White, but was suppressed in Vakara Blue. Together with the finding that anthocyanin accumulates along leaf margins in the OY-W–infected Vakara Blue (Fig. 1c, 3b), these data suggest that anthocyanin may be responsible for the suppression of the leaf cell death.

However, these experiments cannot exclude the possibility that this finding might be dependent on the genetic background of *Petunia* in addition to anthocyanin accumulation. To test the hypothesis that anthocyanin accumulation contributes to reduce cell death in phytoplasma-infected leaves, we used *Arabidopsis* wild type (WT) and an anthocyanin-deficient mutant (*chs*) for the trypan blue staining. Entire surfaces along leaf veins in both infected WT and infected *chs* were darkly stained (Fig. 3i). However, the statistical analyses of the staining intensity revealed a significantly high number of dead cells in infected *chs* compared with infected WT (Fig. 3j).

Additionally, to assess the effects of anthocyanin on the accumulation of phytoplasma, we quantified the titer of phytoplasma in WT and two anthocyanin-deficient mutants, *chs* and *dfr*, infected with OY-W after 3 weeks. However, there were no significant differences between the WT and the mutants (Fig. 4).

Sugar accumulation during phytoplasma infection. Recent studies revealed that sucrose is associated with the accumulation of anthocyanins, in addition to high light intensity and mineral depletion[27,28]. Additionally, previous reports have shown that phytoplasma infection affects the sugar content[33–36]. However, the relationship between anthocyanin synthesis and the sugar accumulation induced by phytoplasma infection remains unknown. Therefore, to examine this relationship, we measured the fructose, glucose, sucrose, and trehalose contents of healthy and OY-W infected leaves of Vakara Blue and Vakara White, which were subjected to the same experimental condition as those shown in Fig. 3-a, -b, -e, and -f. In both OY-W–infected Vakara Blue and Vakara White leaves, all sugars accumulated to a greater extent than those in the respective healthy leaves (Table 1, Fig. 5). Fructose and glucose contents in infected leaves were higher than those in healthy leaves by 10- to 40-fold. In particular, the sucrose contents of OY-W–infected leaves of both Vakara Blue and Vakara White were much higher than those of healthy leaves, by ~1000-fold (Table 1, Fig. 5). These results showed that the significant elevation of sugars in response to phytoplasma infection occurred independent of anthocyanin accumulation.

Discussion

In this study, we demonstrated the activation of the anthocyanin biosynthesis in response to OY-W phytoplasma infection, resulting in purple top symptoms. To our knowledge, this is the first study at the molecular level to show that purple-coloration symptoms in phytoplasma-infected plants are caused by anthocyanin biosynthesis, based on the following evidence. First, the *Arabidopsis* mutant *chs* leaves did not exhibit purple coloration following OY-W

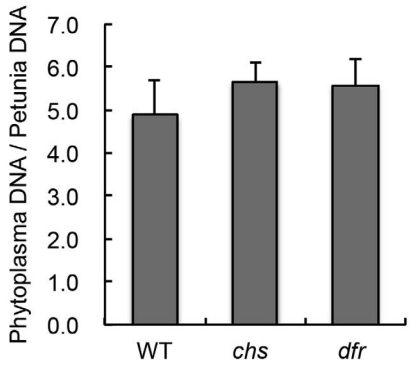

Figure 4 | The effect of anthocyanin on phytoplasma accumulation. Phytoplasma accumulation in *Arabidopsis* plants with or without anthocyanin biosynthesis. The relative levels of phytoplasma accumulations in *Arabidopsis* wild type, *chs*, and *dfr* were detected by real-time PCR for OY-W *tuf B* gene. *Arabidopsis β-tubulin* gene was used for normalization.

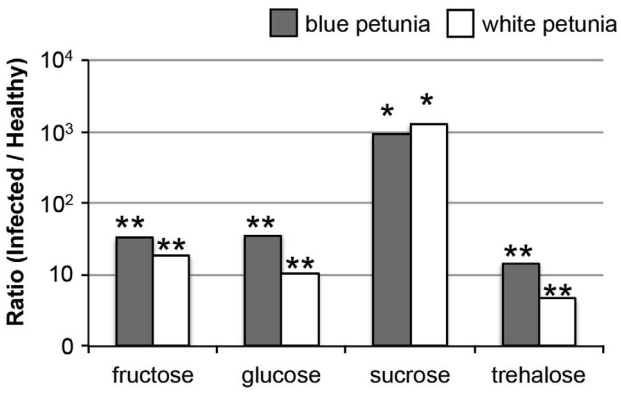

Figure 5 | The ratio of sugar contents in infected leaves to those in healthy leaves. The graphs were visualized from the ratio (Infected/Healthy) data of table 1 with displayed on a log10 scale.

phytoplasma infection (Fig. 2a). Second, the OY-W phytoplasma infection of *Arabidopsis* and blue *Petunia* plants induced significant upregulation of both *CHS* and *DFR*, which are involved in anthocyanin biosynthesis (Fig. 2b). Together, these data revealed that OY-W phytoplasma infection activates the anthocyanin biosynthesis pathway in host plant leaves, resulting in a purple coloration. Furthermore, we found no association between the area of purple coloration and phytoplasma distribution (Fig. 1d). This result suggests that the induction of anthocyanin accumulation does not correlate with phytoplasma titer.

Our studies found that phytoplasma infection induced a high number of cell death in *chs* leaves in compared to WT leaves (Fig. 3j). This result suggests that flavonoids including anthocyanins could reduce cell death caused by infection. Cell death by infection occurred in the leaf vein and the leaf margin (Fig. 3). Leaf vein necrosis was observed in both infected *Petunia* and infected *Arabidopsis* (Fig. 3d, 3h, 3i). Phytoplasma diseases generally induce phloem necrosis[3], and OY-W phytoplasma have also been reported to cause phloem necrosis[37]. Therefore, the leaf vein necrosis observed in this study is considered to be the phloem necrosis. On the other hands, the cell death from the leaf edge was observed in infected white *Petunia* (Fig. 3f, 3h). The mechanisms underlying such cell death remain unclear, because, to our knowledge, cell death at leaf margin has never been examined in phytoplasma-infected plants. However, considering the significant high-content sugars in infected leaves (Table 1, Fig. 5), this symptom might be a type of senescence that can be triggered by high sugar content because sugars are known as positive regulators of leaf senescence[38]. Both kinds of cell death were reduced in leaves accumulated with anthocyanins (Fig. 3). By using *Arabidopsis chs* mutant, which cannot generate flavonoids, it was demonstrated that flavonoids is involved in the reduction of leaf cell death. Flavonoids including anthocyanins are known to act as antioxidant molecules[14,16] and have been shown to delay leaf senescence and contribute to the longevity of leaves[20,39,40]. Our findings are consistent with the role of flavonoids as antioxidant molecules in OY-W phytoplasma infected plants.

On the other hand, the accumulation of flavonoids including anthocyanins did not influence phytoplasma titer (Fig. 4). Flavonoids including anthocyanins have long been recognized as defense-related compounds[15,41,42]. In fact, the accumulation of anthocyanins was shown to reduce the susceptibility of tomatoes to *Botrytis cinerea* by altering dynamics of the ROS burst generated by infection[43]. *B. cinerea* is a necrotrophic pathogen that requires the induction of cell death for growth. In contrast, phytoplasma is a biotrophic pathogen, and requires living cells. Therefore, flavonoids-mediated repression of cell death would not affect OY-W phytoplasma propagation. A recent study suggested that anthocyanin biosynthesis inhibits plant basal immunity in *Arabidopsis*[44]. In addition, it has been reported that pathogen attack and host immunity represses anthocyanin accumulation[44–46]. The interaction of host immunity and phytoplasma infection is still unclear, and further studies are needed to determine how anthocyanin biosynthesis affects host plant–phytoplasma interactions.

The abnormal sucrose level in infected leaves (Table 1, Fig. 5) likely contributes to anthocyanin induction for the following reasons. Sugar (such as sucrose, glucose, and fructose)-dependent upregulation of anthocyanin biosynthesis has often been reported, and in particular, the induction of sucrose-specific anthocyanin synthesis

Table 1 | Sugar analysis in healthy and OY-W phytolasma-infected petunia leaves

	Vakara Blue			Vakara White		
	Healthy (μM)	Infected (μM)	Ratio (Infected/Healthy)	Healthy (μM)	Infected (μM)	Ratio (Infected/Healthy)
Fructose	2042.51 (±998.61)	67012.94 (±6216.34)	32.81**	2120.88 (±148)	39536.41 (±5789.14)	18.64**
Glucose	1447.92 (±782.12)	52136.51 (±5399.3)	36.01**	2105.7 (±304.24)	22461.47 (±1599.94)	10.67**
Sucrose	3.78 (±1.7)	3480.69 (±909.82)	920.82*	3.48 (±4.07)	4473.82 (±1192.94)	1284.35*
Trehalose	15.05 (±6.65)	220.37 (±20.04)	14.64**	19.28 (±2.94)	89.86 (±9.39)	4.66**

Significant differences between healthy and infected tissue were indicated as * ($P < 0.05$) or ** ($P < 0.01$).

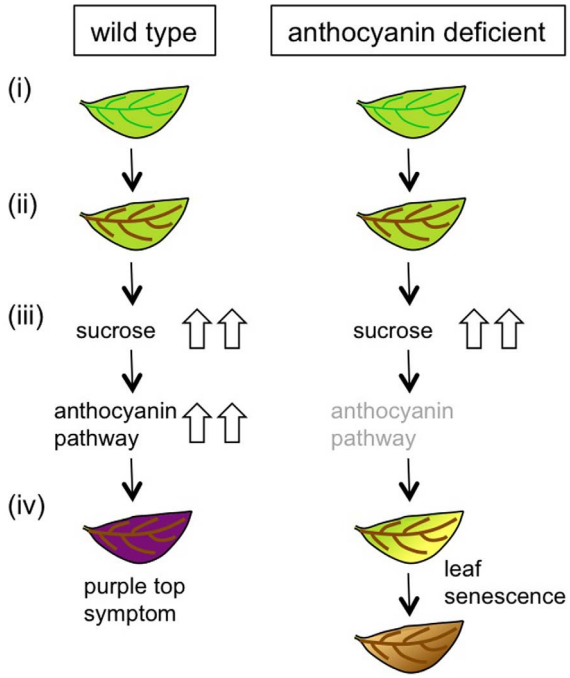

Figure 6 | Schematic model of possible mechanism underlying different leaves symptoms between wild type and anthocyanin deficient mutant in *A. thaliana*. Phytoplasma infections cause phloem necrosis in both wild type and anthocyanin deficient mutant (ii). In those leaves, sucrose concentration is increased at high level by impaired phloem loading (iii). Sucrose accumulation activates the anthocyanin biosynthesis pathway in wild type, resulting in purple top symptoms (iv-left column). In anthocyanin deficient mutant, the leaf shows yellowing symptom and dies earlier than wild type (iv-right column). (Drawings by Misako Himeno).

has been also demonstrated[27,28]. This study revealed that the concentration of sucrose in infected purpling leaves was ~1000-fold higher than that in healthy control plants (Table 1, Fig. 5). The finding that the sucrose concentration in the infected leaves of white *Petunia*, Vakara White, was also significantly increased suggests that the sucrose increment is an upstream signal of anthocyanin accumulation or occurs via an anthocyanin-independent pathway. It has been shown that 15 mM exogenous sucrose was sufficient to enhance anthocyanin accumulation in *Arabidopsis* seedlings[28], however, under the same conditions, the absorbed sucrose concentration inside plant tissue has not been investigated. In this study, the sucrose concentration in infected purpling leaves was increased to 3.5 mM (Table 1), while that in control leaves was 3.8 μM. This concentration inside the leaves may be sufficient to induce anthocyanin synthesis. Collectively, our findings suggest that sucrose is a factor in anthocyanin induction during phytoplasma infection.

In this study, the necrosis of leaf veins was observed in OY-W phytoplasma infected leaves of both *Arabidopsis* and *Petunia* (Fig. 3). Numerous previous studies have suggested that phloem necrosis due to phytoplasma infection may cause a blockage in phloem transport. For example, metabolomic and transcriptional analyses of several phytoplasma-infected plants provided evidence of the inhibition of phloem loading by phytoplasma infection[31–34,44]. Santi *et al.* showed decreased phloem loading through the inhibition of transport gene expression[47]. Together with these findings, the sucrose accumulation in OY-W infected leaves could be considered as a result of the reduction in phloem loading caused by phloem necrosis (Fig. 6).

Phytoplasma symptoms, such as stunted growth and leaf yellowing, are reported to be associated with phloem necrosis and phloem hyperplasia[37,48–50]. In periwinkle (*Catharanthus roseus* (L.) G. Don) source leaves infected with phytoplasmas, leaf bleaching (yellowing) may result from a high content of carbohydrates[33]. Moreover, leaf yellowing by a stolbur phytoplasma infection was associated with the repression of genes involved in sugar transport[51]. Similarly, the leaf yellowing observed in this study (Fig. 2a and 3f) was likely associated with the abnormal sugar contents due to decreased phloem loading.

Our study revealed that anthocyanin accumulation did not influence phytoplasma growth, as discussed above (Fig. 4). Rather, sucrose upregulation might facilitate the spread of phytoplasma infection, since many insects favor sucrose[52], and insect vectors might be attracted to infected plants. Anthocyanin accumulation may also benefit phytoplasma, because the longevity of purple-colored leaves seems to enhance the preference of sucking insects that transmit disease. Further studies will be required to elucidate the benefits of sucrose and anthocyanin accumulation for phytoplasma survival.

Methods

Plant material and phytoplasma infection. Seeds of *Arabidopsis thaliana*, ecotype Landsberg erecta (Ler) and mutant lines CS84 and CS85 were provided by the Arabidopsis Biological Resource Center (ABRC) (Ohio State University, Columbus, OH). *Petunia hybrida* cultivars, Vakara Blue and Vakara White (Sakata Seeds Ltd, Yokohama, Japan), were used in this study. *A. thaliana* and *P. hybrida* plants were grown in growth chambers with 16-h-light/8-h-dark cycles at 25°C.

A wild strain of onion yellows phytoplasma (OY-W strain) has been maintained in a plant host, *Chrysanthemum coronarium*, using a leafhopper vector, *Macrosteles striifrons* as described previously[37]. Inoculations of *Arabidopsis* and *Petunia* with phytoplasma were performed as described previously[5,53]. Note that the "healthy" plants used in all experiments were fed on by healthy leafhoppers for 1 week.

DNA isolation and OY-W phytoplasma quantification. Total DNA was isolated from phytoplasma-infected tissues using the GENE PREP STAR PI-80X system (KURABO) according to the manufacturer's procedure. The accumulation of phytoplasma DNA was quantified using Thermal Cycler Dice real-time PCR system (TaKaRa) with SYBR Premix ExTaq (TaKaRa). The primer set for phytoplasma detection was designed from the elongation factor Tu gene of OY (*tufB*) as described previously[54]. Results were normalized using *β-tubulin* and *PhGAPDH* as host DNA genes in *A. thaliana* and *P. hybrida*, respectively[53] (Table 2).

RNA isolation and real time quantitative RT-PCR. Total RNA was extracted from leaves using Sepasol–RNA I (Nacalai Tesque, Inc.) according to the manufacturer's protocol. Both DNase treatment and real-time quantitative RT-PCR were carried out

Table 2 | Primers designed in this study

Primer name	Nucleotide sequence (5′-3′)	Target gene	Target organism
aCHS-F	TCGGAAACGTCACATGCATC	*CHS*	*A. thaliana*
aCHS-R	GTCCAGAGAAGGAGCCATGTAAG	*CHS*	*A. thaliana*
aDFR-F	TATCACCGCGCTCTCTCCTATC	*DFR*	*A. thaliana*
aDFR-R	GTCGTCCAAATGCACATACTGTC	*DFR*	*A. thaliana*
btublin-F	TGAAGGAATGGACGAGATGGA	*β-tublin*	*A. thaliana*
btublin-R	TGCAGTTGCGTCTTGGTATTG	*β-tublin*	*A. thaliana*
CHS-F	TGGTGACAGTCGAGGAGTATCG	*CHS*	*P. hybrida*
CHS-R	TAGGTGTGGCTGTTCCAATGG	*CHS*	*P. hybrida*
DFRA-F	CCGAAGTGCTGAAGACAATGG	*DFR*	*P. hybrida*
DFRA-R	TGCATTCTCTTTGCCACTTGC	*DFR*	*P. hybrida*

as described previously[53]. The results were normalized using *β-tubulin* and *PhGAPDH* in *A. thaliana* and *P. hybrida*, respectively. The primer sets designed in this study are shown in Table 2. Each data point represents the mean of at least three biological replicates and three technical replicates.

Trypan blue staining. Trypan blue staining was performed for the detection of cell death. Leaf samples were stained with lactophenol-trypan blue solution[55] and cleared with chloral hydrate solution[56]. Signal intensity was quantified using Image J (National Institutes of Health) as described by Ishii *et al.*[57], and values were normalized based on healthy *A. thaliana* leaves treated with the same trypan blue staining procedure.

Quantification of sugars by LC-TOF-MS. A total of 0.2 g of *Petunia* leaves was homogenized in liquid nitrogen and mixed with 200 µl pure water. After centrifugation, an equal volume of chloroform was added to the supernatant, mixed and centrifuged. The supernatant was stored at −80°C until required for analysis. The samples were diluted 1 : 20 by 75% acetonitrile and then filtered with a 0.2 µm syringe filter prior to injection into LC-TOF-MS.

LC-TOF-MS analysis was performed using an ACQUITY ultra performance liquid chromatographic system (Waters) and a LCT Premier XE system (Waters) equipped with 2.1 mm × 100 mm ACQUITY UPLC BEH Amide column maintained at 40°C and eluted with a two-step gradient at 0.13 ml/min. Mobile phase solutions were 0.25% ammonium water (A) and pure acetonitrile (B). The gradient was initiated with 75% of B, and then reduced to 50% of B in a 10 min linear step. The injection volume was 5 µl and the samples were kept at 4°C throughout the analysis. Spectra were collected in both positive and negative ESI modes over a mass range m/z 50–1000.

Statistical analysis. Data are expressed as the means ± S.D. obtained for at least three independent experiments. Statistical analysis was performed by Welch's t-test because $P < 0.05$ was suggested by the F-test in all statistical analyses. P-values < 0.05 were considered to indicate statistical significance.

1. Lee, I. M., Davis, R. E. & Gundersen-Rindal, D. E. Phytoplasma: phytopathogenic mollicutes. *Annu Rev Microbiol* **54**, 221–255 (2000).
2. Oshima, K., Maejima, K. & Namba, S. Genomic and evolutionary aspects of phytoplasmas. *Front Microbiol* **4**, 230 (2013).
3. Hogenhout, S. *et al.* Phytoplasmas: bacteria that manipulate plants and insects. *Mol Plant Pathol* **9**, 403–423 (2008).
4. Sugio, A. *et al.* Diverse targets of phytoplasma effectors: from plant development to defense against insects. *Annu Rev Phytopathol* **49**, 175–195 (2011).
5. Hoshi, A. *et al.* A unique virulence factor for proliferation and dwarfism in plants identified from a phytopathogenic bacterium. *Proc Natl Acad Sci USA* **106**, 6416–6421 (2009).
6. Sugio, A., Kingdom, H. N., MacLean, A. M., Grieve, V. M. & Hogenhout, S. A. Phytoplasma protein effector SAP11 enhances insect vector reproduction by manipulating plant development and defense hormone biosynthesis. *Proc Natl Acad Sci USA* **108**, E1254–1263 (2011).
7. MacLean, A. *et al.* Phytoplasma effector SAP54 induces indeterminate leaf-like flower development in *Arabidopsis* plants. *Plant Physiol* **157**, (2011).
8. Hogenhout, S. & Loria, R. Virulence mechanisms of Gram-positive plant pathogenic bacteria. *Curr Opin Plant Biol* **11**, 449–456 (2008).
9. Andre, A., Maucourt, M., Moing, A., Rolin, D. & Renaudin, J. Sugar import and phytopathogenicity of *Spiroplasma citri*: glucose and fructose play distinct roles. *Mol Plant-Microbe Interact* **18**, 33–42 (2005).
10. Nault, L. Maize bushy stunt and corn stunt: A comparison of disease symptoms, pathogen host ranges and vectors. *Phytopathol* **70**, 659–662 (1980).
11. Banttari, E., Orr, P. & Preston, D. Purple top as a cause of potato chip discoloration. *Trans ASAE* **33**, 221–226 (1990).
12. Franova, J., Paltrinieri, S., Botti, S., Simkova, M. & Bertaccini, A. Association of phytoplasmas and viruses with malformed clovers. *Folia Microbiol* **49**, 617–624 (2004).
13. Duduk, B. & Bertaccini, A. Corn with symptoms of reddening: New host of stolbur phytoplasma. *Plant Disease* **90**, 1313–1319 (2006).
14. Winkel-Shirley, B. Flavonoid biosynthesis. A colorful model for genetics, biochemistry, cell biology, and biotechnology. *Plant Physiol.* **126**, 485–493 (2001).
15. Treutter, D. Significance of flavonoids in plant resistance and enhancement of their biosynthesis. *Plant Biol* **7**, 581–591 (2005).
16. Gould, K., McKelvie, J. & Markham, K. Do anthocyanins function as antioxidants in leaves? Imaging of H_2O_2 in red and green leaves after mechanical injury. *Plant Cell Environ* **25**, 1261–1269 (2002).
17. Neill, S., Gould, K., Kilmartin, P., Mitchell, K. & Markham, K. Antioxidant activities of red versus green leaves in *Elatostema rugosum*. *Plant Cell Environ* **25**, 539–547 (2002).
18. Nagata, T. *et al.* Levels of active oxygen species are controlled by ascorbic acid and anthocyanin in *Arabidopsis*. *J Agric Food Chem* **51**, 2992–2999 (2003).
19. Feild, T., Lee, D. & Holbrook, N. Why leaves turn red in autumn. The role of anthocyanins in senescing leaves of red-osier dogwood. *Plant Physiol* **127**, 566–574 (2001).
20. Schaberg, P., Murakami, P., Turner, M., Heitz, H. & Hawley, G. Association of red coloration with senescence of sugar maple leaves in autumn. *Trees* **22**, 573–578 (2008).
21. Holton, T. & Cornish, E. Genetics and biochemistry of anthocyanin biosynthesis. *Plant Cell* **7**, 1071–1083 (1995).
22. Grotewold, E. The genetics and biochemistry of floral pigments. *Annu Rev Plant Biol* **57**, 761–780 (2006).
23. Deroles, S. Anthocyanin biosynthesis in plant cell cultures: A potential source of natural colourants. In: Kevin, G., Kevin, D. & Chris, W. (eds) *Anthocyanins: Biosynthesis, functions and applications*. 107–117 (2009).
24. Mendez, M., Jones, D. & Manetas, Y. Enhanced UV-B radiation under field conditions increases anthocyanin and reduces the risk of photoinhibition but does not affect growth in the carnivorous plant *Pinguicula vulgaris*. *New Phytol* **144**, 275–282 (1999).
25. Krol, M. *et al.* Low-temperature stress and photoperiod affect an increased tolerance to photoinhibition in *Pinus banksiana* seedlings. *Can J Bot* **73**, 1119–1127 (1995).
26. Rajendran, L., Ravishankar, G., Venkataraman, L. & Prathiba, K. Anthocyanin production in callus cultures of Daucus carota as influenced by nutrient stress and osmoticum. *Biotechnol Lett* **14**, 707–712 (1992).
27. Teng, S., Keurentjes, J., Bentsink, L., Koornneef, M. & Smeekens, S. Sucrose-specific induction of anthocyanin biosynthesis in *Arabidopsis* requires the *MYB75/PAP1* gene. *Plant Physiol* **139**, 1840–1852 (2005).
28. Solfanelli, C., Poggi, A., Loreti, E., Alpi, A. & Perata, P. Sucrose-specific induction of the anthocyanin biosynthetic pathway in *Arabidopsis*. *Plant Physiol* **140**, 637–646 (2006).
29. Kortekamp, A. Expression analysis of defence-related genes in grapevine leaves after inoculation with a host and a non-host pathogen. *Plant Physiol Biochem* **44**, 58–67 (2006).
30. Miranda, M. *et al.* The transcriptional response of hybrid poplar (*Populus trichocarpa* × *P.deltoides*) to infection by *Melampsora medusae* leaf rust involves induction of flavonoid pathway genes leading to the accumulation of proanthocyanidins. *Mol Plant-Microbe Interact* **20**, 816–831 (2007).
31. Albertazzi, G. *et al.* Gene expression in grapevine cultivars in response to Bois Noir phytoplasma infection. *Plant Science* **176**, 792–804 (2009).
32. Hren, M. *et al.* 'Bois noir' phytoplasma induces significant reprogramming of the leaf transcriptome in the field grown grapevine. *BMC Genomics* **10**, (2009).
33. Lepka, P., Stitt, M., Moll, E. & Seemuller, E. Effect of phytoplasmal infection on concentration and translocation of carbohydrates and amino acids in periwinkle and tobacco. *Physiol Mol Plant Pathol* **55**, 59–68 (1999).
34. Maust, B. *et al.* Changes in carbohydrate metabolism in coconut palms infected with the lethal yellowing phytoplasma. *Phytopathol* **93**, 976–981 (2003).
35. Choi, Y. H. *et al.* Metabolic discrimination of *Catharanthus roseus* leaves infected by phytoplasma using 1H-NMR spectroscopy and multivariate data analysis. *Plant Physiol* **135**, 2398–2410 (2004).
36. Giorno, F., Guerriero, G., Biagetti, M., Ciccotti, A. & Baric, S. Gene expression and biochemical changes of carbohydrate metabolism in *in vitro* micro-propagated apple plantlets infected by '*Candidatus* Phytoplasma mali'. *Plant Physiol Biochem* **70**, 311–317 (2013).
37. Oshima, K. *et al.* Isolation and characterization of derivative lines of the onion yellows phytoplasma that do not cause stunting or phloem hyperplasia. *Phytopathol* **91**, 1024–1029 (2001).
38. Wingler, A., Purdy, S., MacLean, J. A. & Pourtau, N. The role of sugars in integrating environmental signals during the regulation of leaf senescence. *J Exp Bot* **57**, 391–399 (2006).
39. Park, J., Canam, T., Kang, K., Unda, F. & Mansfield, S. Sucrose phosphate synthase expression influences poplar phenology. *Tree Physiol* **29**, 937–946 (2009).
40. Tallis, M. J. *et al.* The transcriptome of *Populus* in elevated CO_2 reveals increased anthocyanin biosynthesis during delayed autumnal senescence. *New Phytol* **186**, 415–428 (2010).
41. Dixon, R., Harrison, M. & Lamb, C. Early events in the activation of plant defense responses. *Annu Rev Phytopathol* **32**, 479–501 (1994).
42. Field, B., Jordan, F. & Osbourn, A. First encounters - deployment of defence-related natural products by plants. *New Phytol* **172**, 193–207 (2006).
43. Zhang, Y. *et al.* Anthocyanins double the shelf life of tomatoes by delaying overripening and reducing susceptibility to gray mold. *Curr Biol* **23**, 1094–1100 (2013).
44. Serrano, M. *et al.* Repression of sucrose/ultraviolet B light-induced flavonoid accumulation in microbe-associated molecular pattern-triggered immunity in *Arabidopsis*. *Plant Physiol* **158**, 408–422 (2012).
45. McLusky, S. *et al.* Cell wall alterations and localized accumulation of feruloyl-3′-methoxytyramine in onion epidermis at sites of attempted penetration by *Botrytis allii* are associated with actin polarisation, peroxidase activity and suppression of flavonoid biosynthesis. *Plant J* **17**, 523–534 (1999).
46. Schenke, D., Böttcher, C. & Scheel, D. Crosstalk between abiotic ultraviolet-B stress and biotic (flg22) stress signalling in *Arabidopsis* prevents flavonol accumulation in favor of pathogen defence compound production. *Plant Cell Environ* **34**, 1849–1864 (2011).
47. Santi, S., Grisan, S., Pierasco, A., De Marco, F. & Musetti, R. Laser microdissection of grapevine leaf phloem infected by stolbur reveals site-specific gene responses associated to sucrose transport and metabolism. *Plant Cell Environ* **36**, 343–355 (2013).
48. Braun, E. & Sinclair, W. Histopathology of phloem necrosis in *Ulmus americana*. *Phytopathol* **66**, 598–607 (1976).

49. Schneider, H. Indicator hosts for pear decline: Symptomatology, histopathology, and distribution of mycoplasmalike organisms in leaf veins. *Phytopathol* **67**, 592–601 (1977).
50. Uehara, T. *et al.* Histopathological studies on two symptom types of phytoplasma associated with lettuce yellows. *Annu Phytopathol Soc Jpn* **65**, 465–469. (1999).
51. Jagoueix-Eveillard, S. *et al. Catharanthus roseus* genes regulated differentially by mollicute infections. *Mol Plant-Microbe Interact* **14**, 225–233 (2001).
52. Chapman, R. F. Contact chemoreception in feeding by phytophagous insects. *Annu Rev Entomol* **48**, 455–484 (2003).
53. Himeno, M. *et al.* Unique morphological changes in plant pathogenic phytoplasma-infected petunia flowers are related to transcriptional regulation of floral homeotic genes in an organ-specific manner. *Plant J* **67**, 971–979 (2011).
54. Oshima, K. *et al.* Dramatic transcriptional changes in an intracellular parasite enable host switching between plant and insect. *PLoS One* **6** (2011).
55. Rate, D., Cuenca, J., Bowman, G., Guttman, D. & Greenberg, J. The gain-of-function *Arabidopsis acd6* mutant reveals novel regulation and function of the salicylic acid signaling pathway in controlling cell death, defenses, and cell growth. *Plant Cell* **11**, 1695–1708 (1999).
56. Komatsu, K. *et al.* Viral-induced systemic necrosis in plants involves both programmed cell death and the inhibition of viral multiplication, which are regulated by independent pathways. *Mol Plant-Microbe Interact* **23**, 283–293 (2010).
57. Ishii, Y. *et al.* In the non-insect-transmissible line of onion yellows phytoplasma (OY-NIM), the plasmid-encoded transmembrane protein ORF3 lacks the major promoter region. *Microbiol* **155**, 2058–2067 (2009).

Acknowledgments

This work was supported by Grants-in-Aid for Scientific Research from the Japan Society for the Promotion of Science (category "s" of Scientific Research Grant 25221201), by the Funding Program for Next Generation World-Leading Researchers (project: GS005) initiated by the Council for Science and Technology Policy (CSTP), and by the Program for Promotion of Basic Research Activities for Innovative Bioscience (PROBRAIN).

Author contributions

M.H., K.M., Y.Y., K.O. and S.N. designed research; M.H., Y.K. and T.Y. performed research; M.H. and K.O., analyzed data; and M.H. wrote the paper. All authors discussed the results and commented on the manuscript.

Additional information

Competing financial interests: The authors declare no competing financial interests.

How to cite this article: Himeno, M. *et al.* Purple top symptoms are associated with reduction of leaf cell death in phytoplasma-infected plants. *Sci. Rep.* **4**, 4111; DOI:10.1038/srep04111 (2014).